

Shape Factor and Shape Optimization for a periodic array of isothermal pipes

Marios M. Fyrillas*
Department of Mechanical Engineering
Frederick University, 1303 Nicosia, Cyprus

December 29, 2009

Abstract

We address the problem of two-dimensional heat conduction in a solid slab embedded with a periodic array of isothermal pipes of general cross section. The objective of this work is two-fold: to develop a numerical procedure through which we can obtain the Shape Factor associated with a given configuration and, to develop a numerical Shape Optimization algorithm through which we can compute shapes that extremize the transport rate. The Shape Factor is obtained by first transforming the periodic array of pipes into a periodic array of strips using the generalized Schwarz-Christoffel transformation and, subsequently, by developing an integral equation of the first kind for the temperature gradient using the boundary element method. The integral equation is solved both numerically and analytically/asymptotically with excellent agreement between the results. The Shape Optimization problems, which are formulated with respect to the parameters of the generalized Schwarz-Christoffel transformation, are solved numerically to compute the shape that maximizes the cross-sectional area and the shape that minimizes the perimeter of the cross-section, given the Shape Factor and the distance between two consecutive pipes. It is inferred that the problems are adjoint to the transport rate minimization and transport rate maximization problems, respectively. The optimal shapes are computed numerically and validated with available analytical and numerical results for a single pipe. Furthermore, motivated by the analytical result, we propose a parametric set of equations that describe well the optimal shapes. The versatility of the Laplace equation suggests that similar formulations have applications in continuum mechanics, electricity, hydraulics and drug reduction.

Keywords

Shape Optimization; Solid slab with periodic array of pipes/strips; Heat Conduction, Shape Factor; generalized Schwarz-Christoffel transformation; Laplace equation.

*E-mail: m.fyrillas@frederick.ac.cy

Nomenclature

A	cross-sectional area of a pipe
G	Green's function
H	one half the thickness of the slab
L	distance between two consecutive pipes (period)
P	length of the perimeter of the cross-sectional area of a pipe
S	Shape Factor
T	temperature
W	width of a pipe
w	dimensionless width of a pipe
x, y	coordinates of the physical plane
z	complex coordinate of the physical plane
z_i	vertices in the physical plane
<i>Greek symbols</i>	
α_i	turning angles
ξ, η	coordinates of the transformed domain
w	complex coordinate of the transformed domain
w_i	image of z_i vertices in the transformed domain
<i>Subscripts</i>	
i	related to the i -th vertex
<i>Diacritic</i>	
\wedge	the variable is normalized with w_{N-1}

1 Introduction

In this work we extend the Shape Optimization algorithms developed in [1, 2] to periodic domains. The former publication [1] considers heat conduction in an infinite domain, while the latter publication [2] considers heat conduction in a bounded domain. Here we address the problem of heat conduction in a solid slab embedded with a periodic array of isothermal pipes. The pipes, which can have an arbitrary cross section, are assumed to be symmetric with respect to the midsection of the slab. We present an efficient and accurate numerical procedure for obtaining the Shape Factor [3] associated with any shape and more important, a numerical Shape Optimization algorithm that reveals the optimal shapes that extremize the conduction rate. Both problems are fundamental in many engineering applications: i) in parallel plate compact heat exchangers, the overall heat transfer depends on the shape of the polymer slab [4]; ii) in fin design, although there are a number of optimization strategies to obtain optimum profiles [5, 6, 7], there are no publications that incorporate a two-dimensional heat conduction model [8] iii) in computer technology, the present work has applications in the heat conduction problem due to transistors embedded in a large silicon

substrate [3]; iv) the problem of heat loss from buried, or partially buried, pipes arises in connection with oil lines, powerplant steam and water distribution lines, and underground electrical powerline transmission [9, 10, 11]. Besides heat transfer, many problems in modern science involve domains with an “exotic” boundary shape, where the Laplace equation is ubiquitous. For example, the present formulation has applications in continuum mechanics (torsion [12]), electricity (variable condenser design [13, 14]), hydraulics [15], drug reduction [16, 17], solid propellant rocket motors [18], electromagnetic and acoustical wave guides, conduits commonly used in space vehicles, graphite bricks of gas-cooled nuclear reactors [19, 20, 21]. In all these applications, the results of this work have significant ramifications. On one hand, they provide an efficient and accurate method to obtain a numerical solution to the problem and, more important, a unique methodology that can lead to optimal shapes associated with an objective function and constraints of general form. The latter can become a valuable design tool that can lead to the inception of new, innovative designs.

In order to obtain the Shape Factor [3] we employ conformal mapping techniques [22], and in particular the generalized Schwarz-Christoffel transformation [23, 24, 25, 26]. The physical domain is mapped onto a finite channel with a periodic array of isothermal strips placed at the midsection. The problem in the transformed domain is addressed using the boundary element method and solved numerically as outlined in [27] and asymptotically as outlined in [28].

The main objective and contribution of this work is to develop a numerical Shape Optimization algorithm which would reveal the optimal shapes of a periodic array of pipes such that the conduction rate is extremized, i.e. minimized or maximized. General considerations of optimal shape design can be found in [29, 30] and [31], which however are not directly relevant to this work. Two examples that are closely related to the present work, and in particular to the conduction minimization problem, is the design of a condenser of maximal cross-sectional area at a given capacity [13, 14], and the design of a concrete dam of constant hydraulic gradient [15, 14]. In these publications, the Shape Optimization problems are formulated in an auxiliary plane using conformal mapping techniques and they are solved analytically to obtain expressions for the optimal shapes associated with the transport rate minimization problem. Similar to [2, 1], the advantage of the current formulation is that as it is numerical, it can handle complicated geometrical constraints (linear and/or non-linear equality and/or inequality constraints) and can be extended to bounded domains [2], periodic domains (present work) and other configurations with more complicated boundary conditions (future work). In addition, comparison with the analytical results [2] suggests that a high degree of accuracy can be achieved. In the present work we pose the following two shape optimization problems: i. Find the shape that minimizes the transport rate given the cross-sectional area of the profile and the distance between two consecutive pipes (period), and ii. Find the shape that maximizes the transport rate given the perimeter-length of the cross-sectional profile and the distance between two consecutive pipes (period). Following Fyrillas [2], we pose the following two problems, which it is tempting to infer that they are adjoint to the aforementioned problems:

- Find the shape that maximizes the cross-sectional area given the Shape Factor and the period of the configuration;

- Find the shape that minimizes the perimeter of the cross-sectional profile given the Shape Factor and the period of the configuration.

The Shape Optimization problems are posed as nonlinear programming problems (constrained nonlinear optimization [32, 33]). The objective is to find the constrained maximum/minimum of a scalar function of several variables, which are the parameters of the generalized Schwarz-Christoffel transformation. The Shape Optimization problems are addressed through numerical optimization which can handle complicated geometrical constraints.

In the next Section (§2) we develop a conformal mapping technique where a slab embedded with a periodic array of symmetric pipes, is mapped onto a channel. In Section §3 we address, both analytically (asymptotically) and numerically, the two-dimensional, heat conduction problem in a slab embedded with a periodic array of finite isothermal strips. In Section §4 we pose and solve numerically the two Shape Optimization problems mentioned above. We summarize our findings in the last Section.

2 Conformal transformation of the physical domain into a 2D channel

Consider heat conduction due to a periodic array of isothermal (T_1) symmetric pipes of general cross section, embedded at the center of a solid slab. The upper and lower surfaces of the slab are maintained at temperature T_2 as shown in Figure (1). We non-dimensionalize the lengths with the height H (Figure 2), and the temperature field by subtracting T_2 and diving by the temperature difference $T_1 - T_2$. In addition, because of symmetry, we consider only the upper half of the region (the formulation is also relevant for a period array of isothermal objects embedded in a large, non-conducting substrate) and that the left point of symmetry of one pipe coincides with the origin of the coordinate system. The domain and the parameters associated with the problem are clearly indicated in Figure (2).

Following the analysis in [2], we address this problem through a conformal transformation that maps the physical domain onto a simpler domain, where a solution can be more easily obtained. The transformation is realized by discretizing the boundary of a pipe into straight segments and, by applying the generalized Schwarz-Christoffel transformation [23, 25], we map the physical domain onto a finite channel (Figure 2).

As described by Davis [23] and Floryan [25] an arbitrary channel, bounded by repeated polygonal segments in the physical domain, can be mapped onto a straight channel in the computational domain using the generalized Schwarz-Christoffel transformation (Figure 2)

$$\frac{dz}{dw} = R \prod_{l=-\infty}^{l=\infty} \prod_{j=0}^{j=N} \left(\sinh \left[\frac{\pi}{2h} (w - w_j - lw_N) \right] \right)^{\alpha_j}, \quad (1)$$

where the inner product identifies the number of elements (N) of the shape, and the infinite, outer product the periodic nature of the domain. In the above transformation w_j are the images of the z_j vertices (Figure 2), $\pi\alpha_j$ are the turning angles which are taken to be positive for a clockwise rotation, α_0 and α_N are defined with respect to the x -axis, R is a

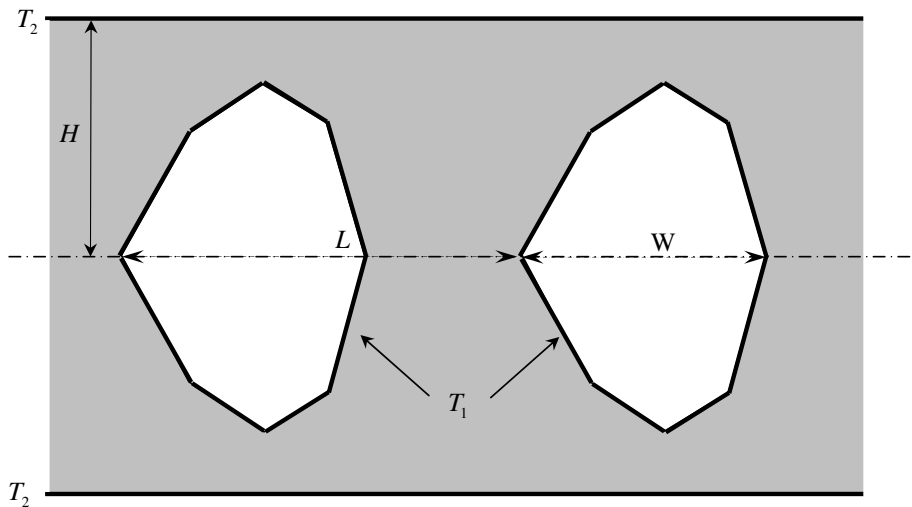


Figure 1: Schematic representation of the physical problem. The surfaces of the slab are kept at a constant temperature T_2 and the distance between them is $2H$. At the mid-distance there is a two-dimensional, periodic array of isothermal symmetric pipes, of general cross section. The width of the pipes is W and the distance between two successive pipes is L . The pipes are kept at temperature T_1 .

complex constant, and h is the height of the channel in the transformed domain taken to be equal to 1. The latter is achieved by requiring that the upper wall of the physical plane, i.e. the line $z = i$, transforms to $w = i$. For the configurations we consider R is a real number, hence:

$$R = \frac{1}{\text{Im}[z[i; \boldsymbol{\alpha}]]}. \quad (2)$$

In addition

$$\sum_{j=0}^N \alpha_j = 0 \text{ and } \alpha_N = 0. \quad (3)$$

The transformation is defined uniquely by choosing an arbitrary point [24, 25]. This is achieved by placing the origin of the transformed domain at the origin of the physical domain ($z_0 = w_0 = 0$). In view of these choices and upon integration the transformation takes the form

$$z[w; \boldsymbol{\alpha}] = R \int_0^w \prod_{l=-\infty}^{l=\infty} \prod_{j=0}^{j=N} \left(\sinh \left[\frac{\pi}{2} (w' - w_j - lw_N) \right] \right)^{\alpha_j} dw', \quad (4)$$

where $\boldsymbol{\alpha}$ represents the $N+1$ -tuple $(\alpha_0, \alpha_1, \alpha_2, \dots, \alpha_N)$.

The parameters w_j , with the exception of w_0 , of the transformation (4) do not appear explicitly but given the physical domain, and hence the angles $\pi\alpha_j$, a system of non-linear equations must be solved for the unknown parameters [23].

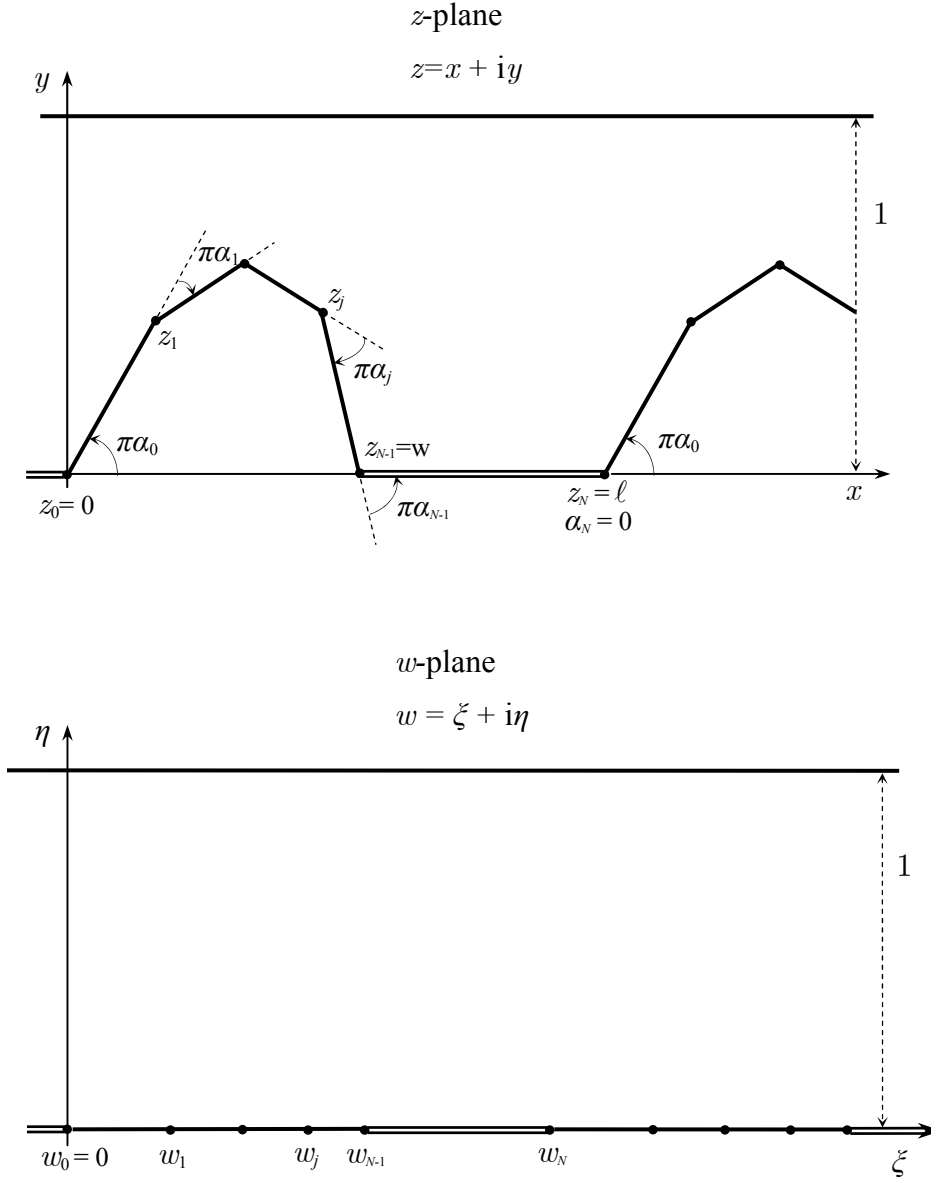


Figure 2: Mapping of the physical domain onto the upper-half plane using the generalized Schwarz-Christoffel transformation (equation 4). The lengths have been non-dimensionalized with the height H , i.e. $\ell = L/H$ and $w=W/H$.

Here we should point out that the optimization problems that we will address in Section §4, similar to the ones formulated in [2], are inverse problems. Whereas the classical approach is to compute the w_j s, in the Shape Optimization we will need to compute the α_j s, while the w_j s will be defined a priori.

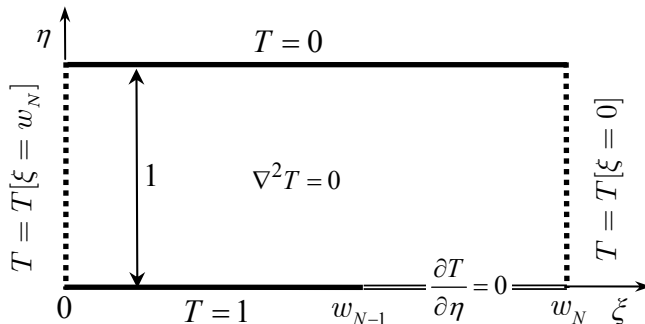


Figure 3: Schematic representation of the model problem along with boundary conditions. The Neumann boundary is dictated by the symmetry of the pipe.

3 Heat conduction due to a periodic array of isothermal strips

The basic problem associated with our analysis is that of heat conduction in a slab where the upper and lower surfaces are kept at a constant temperature $T = 0$. At the center of the slab there is a two-dimensional (infinite span), periodic array of isothermal strips of length w_{N-1} and period w_N , which are kept at temperature $T = 1$. At steady-state, the temperature distribution is governed by the Laplace equation $\nabla^2 T = 0$. In view of the symmetry of the problem in the η direction and periodicity in the ξ direction, the boundary conditions are as follows:

$$\text{On } \eta = 0 \quad \begin{cases} T[\xi] = 1 & \text{along } 0 \leq \xi \leq w_{N-1} \\ \frac{\partial T}{\partial \eta}[\xi] = 0 & \text{along } w_{N-1} < \xi < w_N \end{cases} \quad (5)$$

$$\text{On } \eta = 1 \quad T = 0$$

$$T[\xi = 0, \eta] = T[\xi = w_N, \eta].$$

The mathematical model along with the boundary conditions are shown in Figure (3).

In the next section, using the boundary element method [27], we obtain a Fredholm integral equation of the first kind for the temperature gradient along a single strip. This is solved numerically, and asymptotically for some limiting cases.

3.1 Boundary element formulation and solution

The objective of this section is to determine, as a function of w_{N-1} and w_N , the conduction rate (transport rate) from a single pipe. Equivalently, we define the Shape Factor (S) [3] associated with a single strip of span z :

$$S = -z w_{N-1} \int_0^1 \frac{\partial T[\hat{\xi}, \eta = 0]}{\partial \eta} d\hat{\xi}, \quad (6)$$

where $\hat{\xi} = \xi/w_{N-1}$. Note that we only consider the upper-half of the domain because of symmetry.

We can recast the problem into an integral form along the boundary $\eta = 0$ by applying Green's theorem [34, 27]. An appropriate Green's function is that associated with a periodic array of sources of period w_N located along an insulated, lower surface and a Dirichlet boundary condition along the upper surface:

$$\begin{aligned} \frac{\partial G}{\partial \eta}[\xi', \eta' = 0] &= \sum_{m=-\infty}^{m=\infty} \delta[\xi' - \xi + m w_N] = \frac{1}{w_N} \sum_{k=-\infty}^{k=\infty} e^{2\pi i k(\xi' - \xi)/w_N} \\ G[\xi', \eta' = 1] &= 0. \end{aligned} \quad (7)$$

The Green's function is derived in Appendix A and repeated here for ready reference; when evaluated at $\eta' = 0$ we obtain (equation 22):

$$G[\hat{\xi}' - \hat{\xi}, \eta' = 0] = - \left(\frac{1}{w_N} + \frac{1}{\pi} \sum_{m=1}^{\infty} \frac{1}{m} \tanh [2\pi m/w_N] \cos [2\pi m w_{N-1}(\hat{\xi}' - \hat{\xi})/w_N] \right), \quad (8)$$

where similar to $\hat{\xi}$, we define $\hat{\xi}' = \xi'/w_{N-1}$. Introducing above Green's function into Green's theorem yields:

$$T[\hat{\xi}, \eta = 0] = w_{N-1} \int_0^1 \frac{\partial T[\hat{\xi}', \eta' = 0]}{\partial \eta'} G[\hat{\xi}' - \hat{\xi}, \eta' = 0] d\hat{\xi}',$$

which when evaluated along the strip $0 \leq \hat{\xi} \leq 1$ we obtain an integral equation for the temperature gradient:

$$1 = w_{N-1} \int_0^1 \frac{\partial T[\hat{\xi}', \eta' = 0]}{\partial \eta'} G[\hat{\xi}' - \hat{\xi}, \eta' = 0] d\hat{\xi}' \quad (9)$$

This integral equation is solved numerically using the collocation boundary element method, i.e. the local basis functions are step functions, where the boundary ($0 \leq \hat{\xi} \leq 1$) is discretized into segments (boundary elements) and it is assumed that the unknown function is constant over each element [28, 27]. In addition, we use Kummer's method [35, 36] to accelerate the convergence of the infinite summation in the Green's function (8) using the asymptotic result (12). This approach has been recently applied to address conduction problems in rectangular plates [37], where the solution may have very slowly convergent series, and is analogous to an Ewald summation method [38]. In Figures (4a) and (4b) we show a contour-plot and a 3D-plot of the numerical solution, respectively.

In the next sections, we obtain asymptotic results of the integral equation for a number of cases.

3.1.1 Asymptotic result for large period ($w_N \rightarrow \infty$)

For large w_N , the integral equation (9) must simplify to the integral equation obtained by Fyrrillas [2] for the case of heat conduction due to an isothermal strip. This is justified in

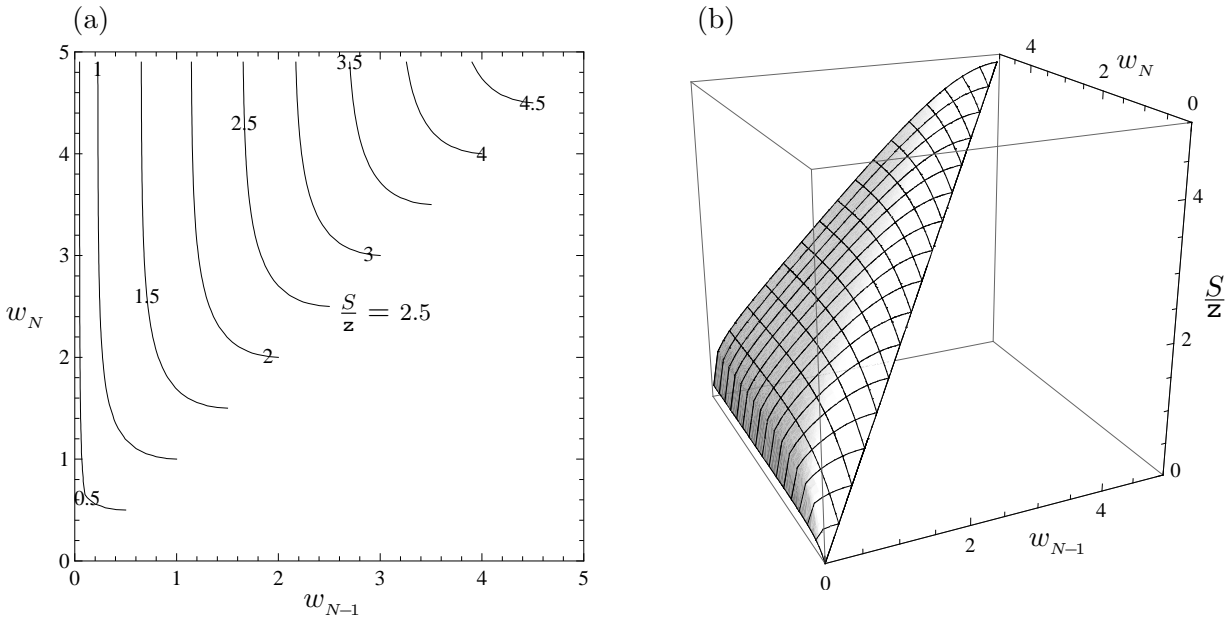


Figure 4: Computed values of the Shape Factor (S/z) as a function of w_N and w_{N-1} . In Figure (a) we show a contour-plot of the Shape Factor, for the values indicated on the figure. In Figure (b) we show a 3-D plot of the Shape Factor. For large values of w_N , the Shape Factor depends only on w_{N-1} (equation 10).

Appendix B where it is shown that the infinite summation in the Green's function (equation 8) is equivalent to a cosine transform in the limit $w_N \rightarrow \infty$. Hence, for large values of w_N the Shape Factor is independent of w_N and depends only on w_{N-1} , i.e. $S[w_N \rightarrow \infty, w_{N-1}] = S[w_{N-1}]$. In Figures (4, 5a), it is shown that the above asymptotic value is attained even for relatively small values of w_N [2, 27].

If we further assume that $w_{N-1} \ll 1$, the Shape Factor is equal to (see equation 9 in [2])

$$S[w_N \rightarrow \infty, w_{N-1} \ll 1] = -\frac{z \pi}{w_{N-1} \ln[\pi w_{N-1}/16]}, \quad (10)$$

which is shown as a dot-dashed curve in Figure (5).

An asymptotic result that was omitted in reference [2], is heat conduction from an isothermal, semi-infinite strip between two parallel, isothermal, flat plates, i.e. ($w_{N-1} \rightarrow \infty$). In fact, an analytical solution can be achieved by first transforming the domain into a semi-infinite slab using the transformation $\log[\coth[z/2]]$ (transformation from an infinite strip with a semi-infinite cut into a semi-infinite strip, C-4, pg 211, [40]), and then transforming the semi-infinite slab to the upper half-plane using the ‘‘cosh’’ transformation (transformation A-3, pg 206, [40]). The solution in the upper-half plane is provided in [40] (pg 243, exercise 7). The temperature gradient can be obtained using the properties of conformal mapping as

$$\frac{\partial T[\xi', \eta' = 0]}{\partial \eta'} = -\frac{1}{\sqrt{1 - \exp[-\pi \xi']}},$$

which suggests that for any $\xi \geq 0$

$$\int_0^\infty \frac{1}{\sqrt{1 - \exp[-\pi \xi']}} \ln \left[\coth \left[\frac{1}{4} \pi |\xi - \xi'| \right] \right] d\xi' = \pi.$$

For large values of ξ' the temperature gradient is equal to $\partial T[\xi', \eta' = 0]/\partial \eta' = -1$, in agreement with the result of heat conduction between two infinite, isothermal, flat plates.

3.1.2 The case $w_N = w_{N-1}$

When $w_N = w_{N-1}$, i.e. heat conduction between two infinite, isothermal, flat plates, we obtain the trivial solution $\partial T[\hat{\xi}', \eta' = 0]/\partial \eta' = -1$ and the Shape Factor is equal to

$$S[w_N = w_{N-1}] = z w_{N-1}, \quad (11)$$

3.1.3 Asymptotic result for small period ($w_N \ll 1$)

For sufficiently small w_N , the term $\tanh[2\pi m/w_N] \approx 1$ and the infinite sum in equation (8) can be replaced by [39]

$$\sum_{m=1}^{\infty} \frac{1}{m} \cos \left[2\pi m w_{N-1} (\hat{\xi}' - \hat{\xi})/w_N \right] = -\ln \left[2 \sin[\pi w_{N-1} |\hat{\xi}' - \hat{\xi}|/w_N] \right]. \quad (12)$$

If we further assume that $w_{N-1} \ll w_N$, then $\sin[\pi w_{N-1} |\hat{\xi}' - \hat{\xi}|/w_N] \approx \pi w_{N-1} |\hat{\xi}' - \hat{\xi}|/w_N$, and the integral equation (9) simplifies to:

$$1 = w_{N-1} \int_0^1 \frac{\partial T[\hat{\xi}', \eta' = 0]}{\partial \eta'} \left(-\frac{1}{w_N} + \frac{1}{\pi} \ln \left[2\pi w_{N-1} |\hat{\xi}' - \hat{\xi}|/w_N \right] \right) d\hat{\xi}'.$$

Assuming a solution of the form [2]

$$\frac{\partial T[\hat{\xi}', \eta' = 0]}{\partial \eta'} = \frac{a_0}{\sqrt{\hat{\xi}'(1 - \hat{\xi}')}},$$

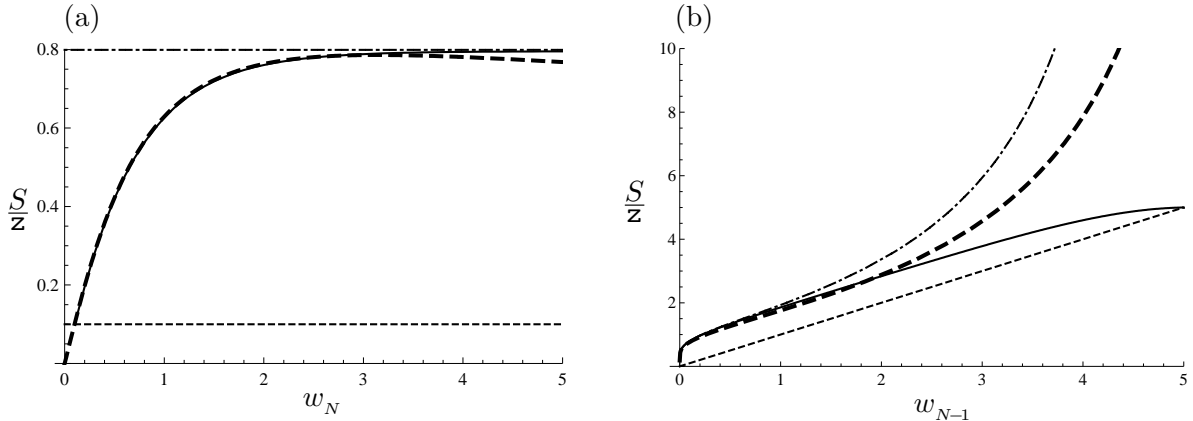


Figure 5: Computed values of the Shape Factor. The solid curves correspond to numerical results and the dashed curves to asymptotic results. The thin-dashed lines correspond to equation (11) valid for $w_N = w_{N-1}$; the thick-dashed curves to equation (13) valid for $w_{N-1} \ll w_N \ll 1$; and the dot-dashed curves to equation (10) valid for $w_N \rightarrow \infty$ and $w_{N-1} \ll 1$. In Figure (a) we show a plot of the Shape Factor as a function of w_N for $w_{N-1} = 0.1$ while in Figure (b), we show a plot of the Shape Factor as a function of w_{N-1} for $w_N = 5$.

reduces the integral equation to an algebraic equation with solution

$$a_0 = \frac{1}{w_{N-1} (\ln[2\pi w_{N-1}/w_N] - \ln[4] - \pi/w_N)}.$$

Hence, for $w_N \ll 1$ and $w_{N-1} \ll w_N$ the Shape Factor is equal to

$$S[w_{N-1} \ll w_N \ll 1] = -\frac{z\pi}{\ln[2\pi w_{N-1}/w_N] - \ln[4] - \pi/w_N}. \quad (13)$$

As shown in Figure (5), there is excellent agreement between the asymptotic results (equations 10, 11 and 13) and the numerical solution. In the next section, based on the findings of the previous sections, we pose two Shape Optimization problems that extremize the transport rate from a periodic array of isothermal pipes.

4 Shape Optimization

The formulation of the Shape Optimization problem, follows along the same lines as the problems formulated by Fyrrillas [2, 1]. We pose the following two shape optimizations problems: i. Find the shape that minimizes the conduction rate, or equivalently the Shape Factor, given the cross-sectional area and the distance (period) between two consecutive pipes and, ii. Find the shape that maximizes the conduction rate, or equivalently the Shape Factor, given the perimeter-length of the cross-sectional profile and the distance (period) between two consecutive pipes. In view of the fact that we do not have an explicit expression for the Shape Factor as a function of all the parameters involved (α , w_N and w_{N-1}), we pose the following two, equivalent problems:

1. Find that shape that maximizes the cross-sectional area given the Shape Factor and the period ℓ associated with the array of pipes,
2. Find the shape that minimizes the perimeter of the cross-sectional profile, given the Shape Factor and the period ℓ associated with the array of pipes.

It is important to note that in the current problem the Shape Factor is a function of two variables, w_N and w_{N-1} . Hence, unlike the single pipe problem formulated in [2], we can not claim monotonicity in order to formulate the optimization problem in terms of w_{N-1} . However, it is tempting to infer that these two problems are adjoint and complimentary (dual) to the conduction rate minimization and the conduction rate maximization problems [41], respectively.

We proceed by expressing w_{N-1} as a function of w_N for a given value of the Shape Factor, which corresponds to a contour in Figure (4a). Hence, we normalize z , w , θ and w_N in equation (4) with respect to w_{N-1}

$$\hat{z}[\hat{w}; \boldsymbol{\alpha}, \hat{w}_N, w_{N-1}] = R \int_0^{\hat{w}} \prod_{l=-\infty}^{l=\infty} \prod_{j=0}^{j=N} \left(\sinh \left[\frac{w_{N-1} \pi}{2} (\hat{w}' - \hat{w}_j - l \hat{w}_N) \right] \right)^{\alpha_j} d\hat{w}'$$

and we define

$$\hat{z}_i[\boldsymbol{\alpha}, \hat{w}_N, w_{N-1}] = R \int_0^{\hat{w}_i} \prod_{l=-\infty}^{l=\infty} \prod_{j=0}^{j=N} \left(\sinh \left[\frac{w_{N-1} \pi}{2} (\hat{w}' - \hat{w}_j - l \hat{w}_N) \right] \right)^{\alpha_j} d\hat{w}'. \quad (14)$$

Here, we clarify the parameters appearing in the above equation:

- The value of R is calculated through equation (2).
- The \hat{w}_j s, with the exception of \hat{w}_N , can be defined a priori; for example equispaced points ($N+1$ -tuple) between 0 and 1.
- As mentioned earlier, the value of w_{N-1} can be expressed as a function of \hat{w}_N , once the value of the Shape Factor is assigned.
- The value of \hat{w}_N can be established by fixing the dimensionless period ℓ of the configuration.

In order to formulate the Shape Optimization problems, we define the dimensionless area associated with the cross-sectional area of a pipe (upper half)

$$A[\boldsymbol{\alpha}, \hat{w}_N, w_{N-1}] = w_{N-1}^2 \sum_{j=0}^{N-2} \frac{\text{Im}[\hat{z}_{j+1} + \hat{z}_j]}{2} \text{Re}[\hat{z}_{j+1} - \hat{z}_j] = \frac{w_{N-1}^2}{2} \sum_{j=0}^{N-2} (\hat{y}_{j+1} + \hat{y}_j)(\hat{x}_{j+1} - \hat{x}_j), \quad (15)$$

and the dimensionless length of the polygonal segments associated with a pipe (upper half)

$$P[\boldsymbol{\alpha}, \hat{w}_N, w_{N-1}] = w_{N-1} \sum_{j=0}^{N-2} |\hat{z}_{j+1} - \hat{z}_j|. \quad (16)$$

Note that the last segment is excluded from the above summations (see Figure 2) as it does not correspond to a segment of a pipe. We proceed to formulate the optimization problems with respect to the area (A) and the length of the perimeter (P).

In view of equation (15), the area maximization problem (transport rate minimization) is formulated as follows:

$$\begin{aligned} \text{maximize} \quad & w_{N-1}^2 \sum_{j=0}^{N-2} (\hat{y}_{j+1} + \hat{y}_j)(\hat{x}_{j+1} - \hat{x}_j) \\ (\boldsymbol{\alpha}, w_N) \end{aligned} \quad (17)$$

subject to the constraints

$$\begin{aligned} \sum_{j=0}^N \alpha_j &= 0 \\ \alpha_N &= 0 \\ w_{N-1} &= w_{N-1} [\hat{w}_N, S] \\ \text{Re}[\hat{z}_N[\alpha_j]] &= \hat{x}_N = \ell/w_{N-1} \\ \text{Im}[\hat{z}_N[\alpha_j]] &= \hat{y}_N = 0. \end{aligned} \quad (18)$$

A similar approach can be employed to define the perimeter-length minimization problem (transport rate maximization). In view of equation (16), the problem is formulated as follows:

$$\begin{aligned} \text{minimize} \quad & w_{N-1} \sum_{j=0}^{N-2} |\hat{z}_{j+1} - \hat{z}_j| \\ (\boldsymbol{\alpha}, w_N) \end{aligned} \quad (19)$$

subject to the constraints

$$\begin{aligned} \sum_{j=0}^N \alpha_j &= 0 \\ \alpha_N &= 0 \\ w_{N-1} &= w_{N-1} [\hat{w}_N, S] \\ \text{Re}[\hat{z}_N[\alpha_j]] &= \hat{x}_N = \ell/w_{N-1} \\ \text{Im}[\hat{z}_N[\alpha_j]] &= \hat{y}_N = 0. \end{aligned} \quad (20)$$

The geometrical constraints (18) and (20) are necessary in view of the domain associated with the problem (see Figures 1 and 2). Note that for large values of w_N (large ℓ) the value of w_{N-1} attains a constant value, independent of w_N (section §3.1.1), and the Shape Optimization problems simplify to the ones formulated by Fyrillas [2]. In the next section we solve numerically the two optimization problems (17) and (19).

4.1 Model calculations

In this work, similar to [2, 1], we have used conformal mapping techniques to formulate the shape optimization problems (17) and (19) as nonlinear programming problems (constrained nonlinear optimization), i.e. find the constrained extremum of a scalar function of several variables, where the variables are the parameters of the generalized Schwarz-Christoffel transformation. Similar to the above references, we employ the Optimization Toolbox of MATLAB [33, 42, 43] to address the Shape Optimization problems under consideration.

In order to evaluate the objective function and the nonlinear constraints, it is required to compute the integral \hat{z}_i (equation 14) which: i) has integrable power-law singularities when $\alpha_j < 0$, ii) it includes an infinite product, and iii) it requires to assume values for the \hat{w}_j s. The former is addressed through Gauss-Jacobi quadrature, as outlined in [44, 45];

The infinite product appearing in the integral can be truncated to a small value without affecting the accuracy due to the exponential decay of the hyperbolic sines [24, 25]; With the exception of w_N , we choose the \hat{w}_j s to be equispaced between 0 and 1 except near large slopes, i.e. when the α_j s are large, where we include some extra points in order to improve the accuracy. The computations were performed on a personal computer and converged without the need to include explicit expressions for the gradient of the objective function and the constraints. For 10 points the simulations converged usually within 15-25 iterations, while a complete calculation did not require more than 10-15 minutes of CPU time. As a starting vector we have used $\boldsymbol{\alpha} = 0$, however the accuracy of the converged solution was verified by repeating the calculation with smaller tolerances and a different starting vector.

In Figure (6) we show the results (points) obtained from the numerical solution of the area maximization problem (transport rate minimization, Shape Optimization problem 17), associated with a Shape Factor value of $S/z = 1.8553$. In the first case (Figure 6a), we consider a large distance between two consecutive pipes ($\ell = 10$), and through numerical optimization we obtain $\hat{w}_N = 10.179$, $A = 0.0895$ and $w_{N-1} = 1.0$. The large value of \hat{w}_N suggests that the problem can be treated as a single pipe (§3.1.1). In fact there is good agreement between numerical (points) and analytical (solid curve) results [15, 14]. In the second case, (Figure 6b) the dimensionless distance between the two pipes is set to $\ell=1.65$ and through numerical optimization we obtain $\hat{w}_N = 1.31$, $A = 0.18$, and $w_{N-1} = 1.49$. Motivated by the analytical result [15, 14], and the curve-fitting proposed by Fyrrillas [2], we perform a least-square fit to the data using the following set of parametric equations

$$\frac{x}{w} = \frac{1}{2} \left(\frac{\ln \left[\frac{p+\cos\theta}{p-\cos\theta} \right]}{\ln \left[\frac{p+1}{p-1} \right]} + 1 \right), \quad \frac{y}{y_{max}} = \frac{\arctan \left[\frac{\sin\theta}{\sqrt{p^2-1}} \right]}{\arctan \left[\frac{1}{\sqrt{p^2-1}} \right]}, \quad (21)$$

where $0 \leq \theta \leq \pi$, and using p as the fitting parameter. The least-square curve (solid curve) fits the data quite well. A comparison between Figures (6a) and (6b), suggests that when the pipes get closer together, the thermal interaction between the isothermal pipes leads to a reduction in the temperature gradient in the region between them, hence the optimal shape becomes elongated in the horizontal direction accompanied by an increase in the cross-sectional area.

In Figure (7) we show the results (points) obtained from the numerical solution of the perimeter-length minimization problem (transport rate maximization, Shape Optimization problem 19) associated with $S/z = 1.8553$. In Figure (a), the dimensionless distance between the two pipes is set to $\ell=10$, and through numerical optimization we obtain $\hat{w}_N = 10.2$, $P = 0.748$ and $w_{N-1} = 1.0$. The large value of \hat{w}_N suggests that the problem can be treated as a single pipe (§3.1.1). In fact there is agreement between the present results and the numerical results for a single pipe (Figure 6b in ref. [2]). In Figure (b) the dimensionless distance between the two pipes is set to $\ell=1.65$ and through numerical optimization we obtain $\hat{w}_N = 1.58$, $P = 0.98$, and $w_{N-1} = 1.32$. Contrary to the previous problem, a comparison between Figures (7a) and (7b) suggests that the reduction in the temperature gradient in the region between two isothermal pipes leads to an optimal shape elongated in the vertical direction accompanied by an increase in the perimeter.

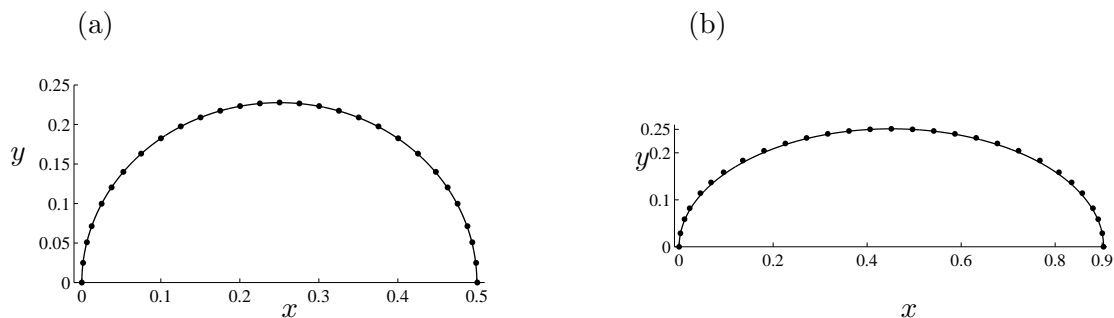


Figure 6: Optimal shape associated with the cross-sectional area maximization problem (transport rate minimization) for $S/z = 1.8553$. Points correspond to numerical results. In Figure (a) the dimensionless distance between the two pipes is set to $\ell=10$ and the solid curve corresponds to analytical results [15, 14]. In Figure (b) the dimensionless distance between the two pipes is set to $\ell=1.65$ and the solid curve corresponds to a least-square fit to equation (21).

In all cases, the set of equations (21) provide an excellent least-square fit to the data (Figure 7). This suggests that the analytical equation by Polubarinova-Kochina [15, 14] is universal, and the complexity rests on finding expressions for p , w and y_{max} through the procedure outlined therein which, however, might be possible only for some simple cases.

5 Conclusions

We have addressed the problem of heat conduction in a solid slab embedded with a periodic array of isothermal, symmetric pipes at the midsection. The upper and lower surfaces of the slab are kept at constant temperature. The formulation is also relevant for a periodic array of isothermal objects placed on an insulated substrate. The heat conduction problem, which is governed by the Laplace equation, is addressed using conformal mapping techniques and in particular the generalized Schwarz-Christoffel transformation. The transformation maps the domain onto a finite channel with a periodic array of isothermal strips. The problem in the transformed domain is addressed using the boundary element method to obtain a

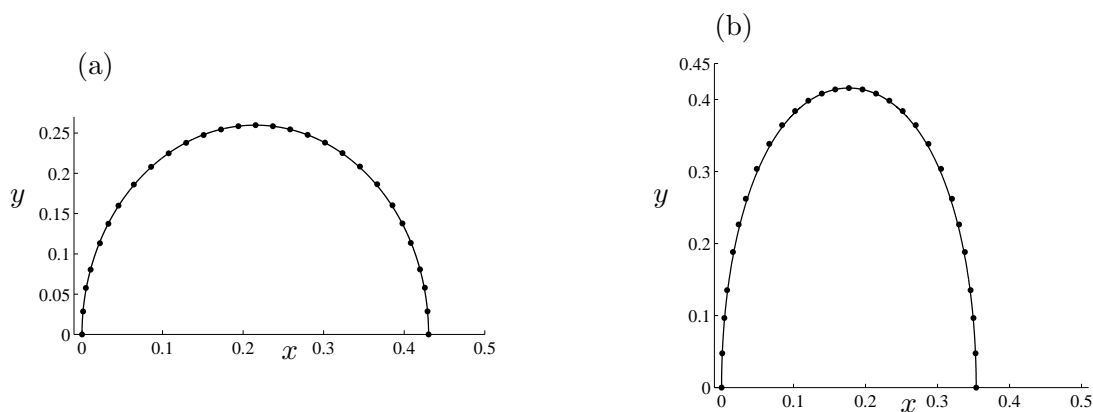


Figure 7: Optimal shape associated with the perimeter-length minimization problem (transport rate maximization) for $S/z = 1.8553$. Points correspond to numerical results while the solid curves to a least-square fit to equation (21). In Figure (a) the dimensionless distance between the two pipes is set to $\ell=10$. In Figure (b) the dimensionless distance between the two pipes is set to $\ell=1.65$.

Fredholm integral equation of the first kind for the temperature gradient along a strip. The integral equation is solved numerically to obtain results for the conduction rate and the Shape Factor. We also obtain asymptotic results which compare well with the numerical result.

Subsequently, given the Shape Factor and the distance between two consecutive pipes, we pose two Shape Optimization problems with the parameters of the generalized Schwarz-Christoffel transformation as the variables of the optimization: find i. the shape that maximizes the cross-sectional area and ii. the shape that minimizes the length of the perimeter. Although it is not proved explicitly, it is expected that these Shape Optimization problems are adjoint to the transport rate minimization and transport rate maximization problems, respectively. The optimization problems are addressed numerically and the results are compared with available analytical and numerical solutions. For large distance between the pipes, the shapes obtained through cross-sectional area maximization and perimeter-length minimization agree with analytical results and numerical results for a single pipe, respectively. For small distance between the pipes, the reduction in the gradient of the temperature due to the proximity of the isothermal pipes leads to flatter shapes for the former

and elevated shapes for the latter. The accuracy of the results and the robustness and the versatility of the formulation offers opportunities for improving the design of a broad range of engineering processes and products.

Acknowledgment.

The work was funded by CHAP Ltd. The author would like to thank Panayiota Konstantinou for providing the proof in Appendix B. The paper is dedicated in the memory of Prof. Donald K. Edwards, an extraordinary teacher and mentor.

A Appendix: Green's Function

In this section we develop the Green's function associated with the Laplace equation and the boundary conditions (equation 7):

$$\begin{aligned} \frac{\partial G}{\partial \eta'}[\xi', \eta' = 0] &= \frac{1}{w_N} \sum_{k=-\infty}^{k=\infty} e^{2\pi i k(\xi' - \xi)/w_N} = \frac{1}{w_N} \left(1 + 2 \sum_{k=1}^{k=\infty} \cos [2\pi k(\xi' - \xi)/w_N] \right) \\ G[\xi', \eta' = 1] &= 0. \end{aligned}$$

We assume a periodic solution of the form

$$G[\xi', \eta'] = A_0 (\eta' - 1) + \sum_{m=1}^{m=\infty} (A_m[\eta'] \cos [2\pi m(\xi' - \xi)/w_N] + B_m[\eta'] \sin [2\pi m(\xi' - \xi)/w_N]).$$

Substituting in the Laplace equation, results to a system of ordinary differential equations which, along with the boundary conditions, leads to the Green's function

$$G[\xi', \eta'] = (\eta' - 1)/w_N + \sum_{m=1}^{m=\infty} \frac{\sinh [2\pi m(\eta' - 1)/w_N]}{\pi m \cosh [2\pi m/w_N]} \cos [2\pi m(\xi' - \xi)/w_N].$$

Evaluating above expression at $\eta' = 0$ we obtain:

$$G[\xi' - \xi, \eta' = 0] = - \left(\frac{1}{w_N} + \frac{1}{\pi} \sum_{m=1}^{\infty} \frac{1}{m} \tanh[2\pi m/w_N] \cos [2\pi m (\xi' - \xi)/w_N] \right). \quad (22)$$

B Appendix: Green's Function in the limit $w_N \rightarrow \infty$

Formally, an integral can be expressed as a Riemann sum as follows:

$$I = \int_0^{\infty} \frac{\tanh[\mathbf{w}]}{\mathbf{w}} \cos [\mathbf{w} \xi] d\mathbf{w} = \lim_{\Delta \mathbf{w} \rightarrow 0} \sum_{i=1}^{\infty} \frac{\tanh[\mathbf{w}_i]}{\mathbf{w}_i} \cos [\mathbf{w}_i \xi] \Delta \mathbf{w}_i.$$

Let $\mathbf{w}_i = 2\pi m/w_N$, where $m = 1, 2, 3, \dots$, then above summation can be expressed as:

$$I = \lim_{w_N \rightarrow \infty} \sum_{m=1}^{\infty} \frac{\tanh[2\pi m/w_N]}{2\pi m/w_N} \cos [2\pi m \xi/w_N] (2\pi/w_N) \Delta m.$$

Simplifying above expression, and realizing that $\Delta m = 1$ because m is an integer, we obtain:

$$\int_0^\infty \frac{\tanh[w]}{w} \cos[w\xi] dw = \lim_{w_N \rightarrow \infty} \sum_{m=1}^{\infty} \frac{\tanh[2\pi m/w_N]}{m} \cos[2\pi m \xi/w_N]. \quad (23)$$

References

- [1] M. M. Fyrillas, Shape optimization for 2D diffusive scalar transport, *Optimization and Engineering to appear*, (<http://dx.doi.org/10.1007/s11081-008-9071-1>).
- [2] M. M. Fyrillas, Heat conduction in a solid slab embedded with a pipe of general cross-section: Shape Factor and Shape Optimization, *Int. J. Eng. Sci.* **46**, 907 (2008).
- [3] F. P. Incropera and D. P. DeWitt, *Fundamentals of Heat and Mass Transfer*, (John Wiley & Sons, 1990).
- [4] F. L. A. Ganzelves and C. W. M. Van Der Geld, The shape factor of conduction in a multiple channel slab and the effect non-uniform temperature, *Int. J. Heat Mass Transfer* **40**, 2493 (1997).
- [5] B. Kundu and P. K. Das, Optimum profile of thin fins with volumetric heat generation: a unified approach, *J. Heat Transfer* **127**, 945 (2005).
- [6] A. R. Kacimov and Yu. V. Obnosov, Explicit rigorous solutions to two-dimensional heat transfer: two-component media and optimization of cooling fins, *Int. J. Heat Mass Transfer*, **40**, 1191 (1997).
- [7] C. Biserni, L. A. O. Rocha and A. Bejan, Inverted fins: geometric optimization of the intrusion into a conducting wall, *Int. J. Heat Mass Transfer* **47**, 2577 (2004).
- [8] A. Aziz, Optimum dimensions of extended surfaces operating in a convective environment, *Appl. Mech. Rev.*, **42**, 155 (1992).
- [9] G. De Mey, Temperature distribution in floor heating systems, *Int. J. Heat Mass Transfer* **23**, 1289 (1980).
- [10] H. H. Bau and S. S. Sadhal, Heat losses from a fluid flowing in a buried pipe, *Int. J. Heat Mass Transfer* **25**, 1621 (1982).
- [11] J. C. Morud and A. Simonsen, Heat Transfer form partially buried pipes, 16th Australasian Fluid Mechanics Conference, (2007).
- [12] E. Romanelli and M.J. Maurizi and P.A. Laura, Torsion of bars of regular polygonal cross sections, *J. Eng. Mech. Div. Proc. Amer. Soc. Civ. Eng.* **paper 8809**, 415 (1972).
- [13] P. M. Morse and H. Feshbach, *Methods of Theoretical Physics, Part II*, McGraw-Hill Science/Engineering/Math, 1953.

- [14] A. Kacimov, Optimal shape of a variable condenser, Proc. R. Soc. Lond. A, **457**, 485 (2001).
- [15] P. Ya Polubarinova-Kochina, *Theory of ground-water movement*, (Princeton University Press 1962).
- [16] D. W. Bechert and M. Bartenwerfer, The viscous flow on surfaces with longitudinal ribs, J. Fluid Mech. **206** 105 (1989).
- [17] P. Luchini, F. Manzo and A. Pozzi, Resistance of a grooved surface to parallel flow and cross-flow, J. Fluid Mech. **513**, 247 (2004).
- [18] J.H. Baltrukonis, *The dynamics of solid propellant rocket motors, Mechanics and Chemistry of Solid Propellants*. (Pergamon Press, 1967).
- [19] P. A. Laura and R. Ercoli, Analysis of unsteady MHD flow in conduits of arbitrary cross section by a complex variable approach, J. Acoust. Soc. America, **51**, 820 (1971).
- [20] P. A. Laura and R. Ercoli, A solution of the unsteady diffusion equation in an arbitrary, doubly connected domain, Nucl. Eng. Design, **23**, 1 (1972).
- [21] P. A. Laura and E. A. Susemihl, Determination of heat flow shape factors for hollow, regular polygonal prisms. Nucl. Eng. Design, **25**, 409 (1973).
- [22] E. Hahne and U. Grigull, Shape factor and shape resistance for steady multidimensional heat conduction, Int. J. Heat Mass Transfer, **18**, 751 (1975).
- [23] R. T. Davis, Numerical methods for coordinate generation based on Schwarz-Christoffel transformation, AIAA Paper No. 79-1463, 4th Computational Fluid Dynamics Conference 180 (1979).
- [24] J. M. Floryan, Conformal-mapping-based coordinate generation method for channel flows, Journal of Computational Physics **58**, 229 (1985).
- [25] J. M. Floryan, Conformal-mapping-based coordinate generation method for flows in periodic configurations, Journal of Computational Physics **62**, 221 (1986).
- [26] M. Brady & C. Pozrikidis, Diffusive transport across irregular and fractal walls, Proc. R. Soc. Lond. A **442**, 571 (1993).
- [27] H. A. Stone, Heat/mass transfer from surface films to shear flows at arbitrary Peclet numbers, Phys. Fluids A **1**, 1112 (1989).
- [28] M. M. Fyrillas, Advection-dispersion mass transport associated with a non-aqueous-phase liquid pool, J. of Fluid Mech. **413**, 49 (2000).
- [29] O. Pironneau, *Optimal shape design for elliptic systems*, (Springer, New York, 1984).
- [30] J. Haslinger and R.A.E. Mokin, *Introduction to Shape Optimization: Theory, Approximation, and Computation*, (SIAM, 2003).

- [31] A. Bejan and S. Lorente, *Design with constructal theory*, (Wiley, 2008).
- [32] R. Fletcher, *Practical Methods of Optimization*, (John Wiley and Sons, 1987).
- [33] *Optimization Toolbox*, The MathWorks Inc., 2000.
- [34] M. D. Greenberg, *Foundations of Applied Mathematics*, (Prentice-Hall, 1978).
- [35] M. Abramowitz and I. Stegun, *Handbook of Mathematical Functions*, (Dover, 1964).
- [36] K. Knopp, *Theory and application of infinite series*, (Blackie & Son, London, 1951).
- [37] J. V. Beck, N. T. Wright, A. Haji-Sheikh, K. D. Cole and E. Amos, Conduction in rectangular plates with boundary temperatures specified, (Int. J. Heat Mass Transfer) **51**, 4676 (2008).
- [38] P. P. Ewald, Die Berechnung optischer und elektrostatischer Gitterpotentiale, Ann. Phys. **64**, 253 (1921).
- [39] W. Magnus and F. Oberhettinger, *Formulas and theorems for the functions of mathematical physics*, (Chelsea Publishing Company, New York, 1949).
- [40] S. Lipschutz, *Theory and Problems of complex variables*, (Schaum's outline series, McGraw-Hill book company, 1974).
- [41] N. B. Il'inksii and A. R. Kacimov, Seepage-limitation optimization of the shape of an irrigation channel by the inverse boundary-value problem method, Fluid Dynamics **19**, 404-410 (1994).
- [42] R. Fletcher and M. J. D. Powell, A rapidly convergent descent method for minimization, Computer Journal **6**, 163 (1963).
- [43] D. Goldfarb, A family of variable metric updates derived by variational means, Mathematics of computing **24**, 23 (1970).
- [44] T. A. Driscoll, *Schwarz-Christoffel Toolbox Users Guide*.
- [45] T. A. Driscoll & L. N. Trefethen, *Schwarz-Christoffel Mapping*, (Cambridge University Press, 2002).